Senescence-associated IL-33 secretion undermines sorafenib efficacy in hepatocellular carcinoma via immune evasion

YU-XIN LIN[1*], HSIEN LIU[2*], WEI-CHIAO LIAO[1,3], YI-CHING WANG[3,4], BO-CHENG ZHANG[1], SHU-WEN WAN[1,3,5], CHIEN-CHIN CHEN[6-9] and CHIH-PENG CHANG[1,3,5]

[1]Department of Microbiology and Immunology, College of Medicine, National Cheng Kung University, Tainan 70101, Taiwan; [2]Division of General Surgery, Department of Surgery, Ditmanson Medical Foundation Chia-Yi Christian Hospital, Chiayi 60002, Taiwan; [3]Institute of Basic Medical Sciences, College of Medicine, National Cheng Kung University, Tainan 70101, Taiwan; [4]Department of Pharmacology, College of Medicine, National Cheng Kung University, Tainan 70101, Taiwan; [5]Center of Infectious Disease and Signaling Research, National Cheng Kung University, Tainan 70101, Taiwan; [6]Department of Pathology, Ditmanson Medical Foundation Chia-Yi Christian Hospital, Chiayi 60002, Taiwan; [7]Department of Cosmetic Science, Chia Nan University of Pharmacy and Science, Tainan 71710, Taiwan; [8]Doctoral Program in Translational Medicine, Rong Hsing Research Center for Translational Medicine, National Chung Hsing University, Taichung 40227, Taiwan; [9]Department of Biotechnology and Bioindustry Sciences, College of Bioscience and Biotechnology, National Cheng Kung University, Tainan 70101, Taiwan

Received July 3, 2025; Accepted August 28, 2025

DOI: 10.3892/or.2025.8987

Abstract. Hepatocellular carcinoma (HCC) is a highly lethal cancer with increasing incidence rates worldwide. The recommended treatments for advanced-stage HCC are sorafenib and regorafenib; however, developing resistance to these medications significantly limits their effectiveness, and the underlying mechanisms are poorly understood. The present study demonstrated that interleukin-33 (IL-33) promotes sorafenib resistance via immune regulation. *In vitro*, western blotting and reverse transcription-quantitative PCR showed that both sorafenib and regorafenib treatments led to an increase in the upregulation and secretion of IL-33 through a positive feedback loop involving the IL-33/transmembrane suppression of tumorigenicity 2 (ST2L) pathway. Senescence-associated β-galactosidase staining and western blotting revealed that sorafenib and regorafenib treatments induce cell senescence in HCC cells. Flow cytometric analysis indicated that he secreted IL-33 enhanced programmed cell death ligand 1 (PD-L1) expression in HCC cells by activating NF-κB pathways in response to the treatments. *In vivo*, a HCC-bearing subcutaneous mouse model revealed that blocking the IL-33 signaling pathway with anti-IL-33 or anti-ST2L neutralizing antibodies, combined with sorafenib, significantly reduced tumor size, growth rate, and weight. Additionally, there was a notable decrease in tumor PD-L1 expression and an increase in intra-tumor $CD8^+$ T cells infiltration. Importantly, the enhanced therapeutic efficacy of the anti-IL-33 treatment in sorafenib-treated HCC-bearing mice was lost in immunocompromised mice. This indicates that the anti-IL-33 neutralizing antibody enhances the antitumor activity of sorafenib by modulating the immune response rather than directly affecting HCC cell proliferation. The findings of the present study suggested that IL-33 plays a role in decreasing the therapeutic effectiveness of sorafenib and regorafenib in HCC cells. The present study highlights the potential of targeting the IL-33/ST2L axis in combination with targeted therapies as a novel strategy to improve the limited efficacy of sorafenib and regorafenib.

Correspondence to: Dr Chien-Chin Chen, Department of Pathology, Ditmanson Medical Foundation Chia-Yi Christian Hospital, 539 Zhongxiao Road, East, Chiayi 60002, Taiwan
E-mail: hlmarkc@gmail.com

Professor Chih-Peng Chang, Department of Microbiology and Immunology, College of Medicine, National Cheng Kung University, 1 University Road, East, Tainan 70101, Taiwan
E-mail: cpchang@mail.ncku.edu.tw

*Contributed equally

Key words: interleukin-33, hepatocellular carcinoma, programmed death ligand 1, regorafenib, sorafenib

Introduction

Hepatocellular carcinoma (HCC) is the leading cause of liver cancer, accounting for an overwhelming 90% of all cases (1). This stark reality highlights the urgent need for proactive prevention, early detection, and treatment measures to combat this formidable disease. The treatment options for patients with HCC depend on their clinical stage (2). Due to the difficulties in early detection and the rapid progression of the disease, numerous patients are diagnosed at advanced stages, and chemotherapeutic agents are the primary form of systemic therapy for these patients (1).

Sorafenib and regorafenib are oral multi-kinase inhibitor that targets several tyrosine kinases, including serine-threonine kinases Raf-1 and B-Raf, which are involved in the MAPK/ERK

pathway (3,4). They are also found to inhibit the platelet-derived growth factor receptor and the vascular endothelial growth factor receptors (VEGFR-2/3) (5). Sorafenib and regorafenib have been approved by the Food and Drug Administration as the first-line and second-line treatments, respectively, to help control tumor angiogenesis and progression in patients with advanced HCC (6,7). While sorafenib and regorafenib are the main systemic therapies for advanced HCC, their effectiveness and application are frequently hindered by severe adverse reactions and the common development of drug resistance (8). Grasping the intricate mechanisms behind this resistance is essential for devising effective strategies to overcome it.

Prolonged use of antitumor drugs can frequently lead to the development of acquired resistance, ultimately undermining the effectiveness of these vital treatments. Multiple critical pathways have been identified that lead to acquired resistance to sorafenib in HCC (9). Importantly, inhibiting T-cell attack in the tumor microenvironment (TME) plays a significant role in promoting drug resistance (10). Programmed death-ligand-1 (PD-L1) is an immune checkpoint protein found on numerous cancer cells that suppresses anticancer immunity by interacting with PD-1 on T cells (11). Overexpression of PD-L1 is found to increase the drug resistance in cisplatin-resistant small cell lung cancer cells, enzalutamide-resistant prostate cancer, and sorafenib-resistant HCC (12-14). Accordingly, PD-1-PD-L1 blockade has been shown to foster $CD8^+$ T-cell infiltration and therapeutic efficacy of sorafenib and regorafenib in tumor-bearing mouse models (15,16). Despite the critical role of PD-L1 in promoting resistance to sorafenib and regorafenib in HCC, the mechanisms underlying PD-L1 upregulation in HCC cells following these drug treatments remain incompletely understood (17).

IL-33 is a member of the IL-1 cytokine family and is widely expressed in various cell types, primarily localized in the nucleus to regulate gene transcription (18). Importantly, IL-33 is able to be released as an alarmin to activate innate and adaptive immune responses by binding its specific receptor ST2L in response to cell stress, pathogen infection, tissue injury and necrotic cell death (19-21). When IL-33 binds to ST2L, this signaling triggers the MyD88-dependent pathways and subsequently induces the activation of activator protein-1 and NF-κB transcription factors, leading to inflammatory gene expression (22,23). This IL-33/ST2L signaling has been observed in accelerating multiple types of cancer progression, including HCC (24,25). In HCC, IL-33/ST2L signaling has been shown to enhance the stemness of HCC cells and alter the immune responses within the TME, leading to accelerated HCC progression (25-27). Notably, our current findings indicate that lung cancer cells treated with cisplatin can release IL-33, creating a positive feedback loop through IL-33/ST2L that limits the efficacy of cisplatin therapy (28). However, it is unclear whether IL-33/ST2L signaling participates in the development of acquired resistance to sorafenib or regorafenib in HCC.

In the present study, it was found that sorafenib and regorafenib treatments induced cell senescence in HCC and promoted the secretion of IL-33 through an IL-33/ST2L positive feedback loop. The secreted IL-33 enhanced PD-L1 expression in HCC cells by activating NF-κB pathways in response to these treatments. Blockage of the IL-33 signaling pathway using anti-IL-33 or anti-ST2L antibodies alongside sorafenib resulted in significant tumor growth reduction in HCC-bearing mice, decreased tumor PD-L1 expression, and increased $CD8^+$ T cell infiltration. However, the increased efficacy was not observed in immunocompromised mice, indicating the crucial role of T cells in the reduced efficacy of sorafenib due to IL-33. The current findings highlight how IL-33 may undermine the effectiveness of sorafenib and regorafenib, suggesting that targeting the IL-33/ST2L axis could enhance therapeutic outcomes in HCC.

Materials and methods

Cell lines and culture. Human hepatoma cell lines Huh-7 cells were obtained from the Bioresource Collection and Research Center. ML-1_{5a} is a mouse hepatoma cell line that was developed from ML-1 cells after being adapted through five generations in BALB/c mice. It originates from the parental ML-1 hepatoma cell line, which was established using liver cells from BALB/c mice that were transformed with the hepatitis B virus X (HBx) gene (29). It was noted that ML-1 is not registered in the Cellosaurus database and therefore does not have an assigned CVCL number. Huh7 and ML-1_{5a} cells were maintained in Dulbecco's Modified Eagle's Medium (DMEM; Gibco; Thermo Fisher Scientific, Inc.) supplemented with 10% fetal bovine serum (FBS; Gibco; Thermo Fisher Scientific, Inc.) and 1% penicillin/streptomycin (Gibco; Thermo Fisher Scientific, Inc.) and cultured at 37˚C with 5% CO_2 in a humidified incubator.

Cell death assay. Huh-7 cells ($5x10^3$ cells/well) were seeded in 96-well plates and treated with sorafenib (cat. no. SC-220125; Santa Cruz Biotechnology) or regorafenib (cat. no. SC-477163; Santa Cruz Biotechnology) at the indicated concentrations for 24 to 96 h. Cell death was assessed using the FITC Annexin V Apoptosis Detection Kit with propidium iodide (cat. no. 640914; BioLegend, Inc.) according to the manufacturer's instructions. Stained cells were analyzed by a CytoFLEX flow cytometer (Beckman Coulter, Inc.), and the acquired data were processed with CytExpert software (version 2.3; Beckman Coulter, Inc.).

Western blot analysis. Cells were harvested and lysed with Cell Lysis Buffer (cat. no. 9803; Cell Signaling Technology, Inc.) supplemented with protease and phosphatase inhibitors. A total of 30 μg of protein lysates, quantified using the Bradford assay, was separated on 12% sodium dodecyl sulfate-polyacrylamide gel electrophoresis and transferred onto polyvinyl difluoride membranes. Membranes were then blocked with 5% skimmed milk in TBST (TBS containing 0.1% Tween-20) for 1 h at room temperature and incubated with specific primary antibodies overnight at 4˚C. The antibodies used were as follows: anti-IL-33 (1:1,000; cat. no. LG3314; Leadgene Biomedical), anti-p16 (1:2,000; cat. no. ab81278; Abcam), anti-p21 (1:1,000; cat. no. 2947S; Cell Signaling Technology, Inc.), anti-PD-L1 (1:1,000; cat. no. 13684S; Cell Signaling Technology, Inc.) and anti-β-actin (1:5,000; cat. no. ab8226-20; Abcam). The membranes were then washed and incubated with horseradish peroxidase-conjugated anti-mouse (1:5,000; cat. no. GTX213111-01; GeneTex, Inc.) or anti-rabbit

(1:5,000; cat. no. GTX213110-01; GeneTex, Inc.) antibodies for 1 h at room temperature. Protein expression was visualized by enhanced chemiluminescence treatment using Western Lightning Plus-ECL (PerkinElmer, Inc.) and Amersham™ Imager 600 (GE Healthcare).

Reverse transcription-quantitative polymerase chain reaction (RT-qPCR). Total RNA was isolated from cells using the Quick-RNA™ MiniPrep kit (cat. no. R1055; Zymo Research), and then 1 μg of total RNA was reverse transcribed into cDNA using M-MLV Reverse Transcriptase (cat. no. LDG0006RF; Leadgene Biomedical) with random primers under the following conditions: 25˚C for 10 min (primer annealing), 42˚C for 60 min (cDNA synthesis), and 70˚C for 10 min (enzyme inactivation). qPCR was performed with the FastStart Universal SYBR Green Master (Rox) (cat. no. 04913850001; Roche Diagnostics) in the StepOnePlus™ Real-Time PCR System (Applied Biosystems; Thermo Fisher Scientific, Inc.). PCR amplification was performed with an initial denaturation at 95˚C for 10 min, followed by 40 cycles consisting of denaturation at 95˚C for 15 sec and combined annealing/extension at 60˚C for 1 min. Gene expression levels were normalized to *ACTB*, and relative expression was calculated using the $2^{-\Delta\Delta Cq}$ method (30). The following primer sequences were used: *IL33* (orward, 5'-CAAAGAAGTTTGCCCCATGT-3' and reverse, 5'-AAGGCAAAGCACTCCACAGT-3'; *CD274* forward, 5'-AAACAATTAGACCTGGCTG-3' and reverse, 5'-TCTTAC CACTCAGGACTTG-3'; and *ACTB* forward, 5'-AAGGAG AAGCTGTGCTACGTCGC-3' and reverse, 5'-AGACAGCAC TGTGTTGGCGTACA-3'.

Cell proliferation analysis. Huh-7 cells ($2x10^5$ cells/well) were seeded in 6-well plates and treated with sorafenib (1 and 10 μM) or regorafenib (10 and 20 μM) at the indicated concentrations for 5 to 7 days. At the end of treatment, cells were trypsinized, collected, and stained with 0.4% Trypan Blue solution (cat. no. T8154; MilliporeSigma) to assess cell viability. Viable (unstained) and non-viable (stained) cells were counted using a hemocytometer under a light microscope. Cell proliferation was determined by quantifying the number of viable cells at each time point.

Senescence-associated β-galactosidase (SA-β-gal) staining. SA-β-gal activity was detected using the Senescence β-Galactosidase Staining Kit (cat. no. 9860; Cell Signaling Technology, Inc.) according to the manufacturer's instructions. Briefly, Huh-7 cells were treated with sorafenib (10 μM) or regorafenib (20 μM) for 4 days. After treatment, cells were washed with PBS and fixed with 1X Fixative Solution for 10-15 min at room temperature. Following two washes with PBS, cells were incubated with β-galactosidase staining solution (pH 6.0) at 37˚C in a sealed container without CO_2 for 1 to 2 days. SA-β-gal-positive cells were observed and imaged using an Olympus BX61 light microscope (Olympus Corporation).

Flow cytometry. To detect surface expression of PD-L1 on Huh-7 cells, the cells were harvested and washed with PBS. The prepared cells were incubated with APC-conjugated anti-human PD-L1 antibody (1:200; cat. no. 393609; BioLegend, Inc.) in staining buffer (2% FBS and 0.1% sodium azide in PBS). The staining was performed for 30 min on ice in the dark, followed by flow cytometric analysis. For immunophenotyping of tumor-infiltrating immune cells isolated from HCC-bearing mice, single-cell suspensions were incubated with fluorochrome-conjugated monoclonal antibodies in staining buffer for 30 min on ice in the dark. The following antibodies were used: FITC anti-mouse CD8a antibody (cat. no. 553031; BD Biosciences), PE anti-mouse CD4 antibody (cat. no. 553049; BD Biosciences) and PE anti-mouse CD152 (CTLA-4) antibody (cat. no. 106305; BioLegend, Inc.). The mean fluorescence intensity and the proportion of cells within a specific gate were detected using a CytoFLEX (Beckman Coulter, Inc.) and analyzed using CytExpert software (Beckman Coulter, Inc.).

HCC-bearing subcutaneous mouse model. A total of 36 male BALB/c mice and 20 male nude mice (8 weeks-old; weighing 25 g) were used. Mice were housed under standard conditions with a temperature of 22±2˚C, relative humidity of 50±5%, a 12/12-h light/dark cycle, and *ad libitum* access to food and water. All animal experiments were conducted in accordance with National Cheng Kung University institutional guidelines for care and use of laboratory animals (approval no. 107130; Tainan, Taiwan). To establish the subcutaneous tumor model, $1x10^6$ ML-1_{5a} cells were injected into the flank of BALB/c or nude mice. Mice harboring HCC allografts were treated with IgG (10 μg/g), sorafenib (10 μg/g), α-IL-33 (10 μg/g; cat. no. LG3314; Leadgene Biomedical), and/or α-ST2L (10 μg/g; cat. no. LGT2105; Leadgene Biomedical) via intraperitoneal (i.p.) injection. Mice received daily i.p. injections of sorafenib from day 7 to day 27. For both monotherapy and combination therapy groups, α-IL-33 or α-ST2L antibodies were administered intraperitoneally on days 7, 14 and 21 post-inoculation. Tumor volume was measured every four days starting on day 5 post-inoculation using a digital caliper and calculated using the formula: V=(length^2 x width)/2. For HCC-bearing nude mice, mice received daily i.p. injections of sorafenib (10 μg/g) from day 4 to day 23, and/or α-IL-33 (10 μg/g) on days 4, 11, and 18. On day 25 or 29 after subcutaneous injection, the HCC-bearing mice were sacrificed, and their solid tumors were removed to determine the tumor weight and infiltrated phenotypes of immune cells by flow cytometry. In the present study, mice were euthanized by carbon dioxide (CO_2) inhalation, with CO_2 introduced into the chamber at a displacement rate of 30% of the chamber volume per min, in accordance with institutional animal care guidelines. Death was confirmed by the absence of respiration and heartbeat, followed by cervical dislocation as a secondary method. All animal experiments were performed between 2020 and 2021.

Immunohistochemistry assay. Formalin-fixed, paraffin-embedded tissue sections (4-μm thick) of mouse HCC tumors were deparaffinized with xylene and rehydrated through a graded series of ethanol solutions. Antigen retrieval was performed by heating the sections in 10 mM citrate buffer (pH 6.0) at 95-100˚C for 10 min. Endogenous peroxidase activity was blocked using 3% hydrogen peroxide for 15 min at room temperature. After washing, the sections were blocked with blocking reagent for 1 h at room temperature and then

incubated with primary antibodies against IL-33 (1:200; cat. no. LG3314; Leadgene Biomedical) and PD-L1 (1:200; cat. no. 13684S; Cell Signaling Technology, Inc.) at 4˚C overnight. The immunoreactions were revealed using the secondary antibody of OneStep Polymer HRP anti-mouse/rat/rabbit Detection System (cat. no. GTX83398; GeneTex, Inc.) and using DAB as chromogen. Nuclei were counterstained with Mayer's hematoxylin (cat. no. HMM125; ScyTek Laboratories Inc.), and slides were subsequently dehydrated and mounted for microscopic analysis.

Enzyme-linked immunosorbent assay (ELISA) assay of IL-6 concentration. Huh7 cells were treated with sorafenib (10 μM) or regorafenib (20 μM) for 72 h, and the culture supernatants were collected. Human IL-6 levels were quantified using a human IL-6 DuoSet ELISA kit (cat. no. DY206; R&D Systems, Inc.) according to the manufacturer's instructions. Optical density (OD) was measured at 450 nm using a SpectraMax iD5 Multi-Mode Microplate Reader (Molecular Devices). The IL-6 concentrations were calculated from a standard curve (Fig. S2).

Correlation analysis of IL33 and CD274 expression in patients with liver hepatocellular carcinoma (LIHC). The correlation between *IL33* and *CD274* expression in LIHC was analyzed using the TIMER2.0 web server (http://timer.cistrome.org/) (31), which integrates RNA-seq data from The Cancer Genome Atlas (TCGA; https://portal.gdc.cancer.gov). Spearman's correlation analysis was performed to assess the association between *IL33* and *CD274* mRNA expression levels in the TCGA-LIHC cohort (Fig. S3).

Statistical analysis. Data are presented as the mean ± standard deviations (SD). Data were analyzed using one-way ANOVA followed by Tukey's post hoc test with GraphPad Prism 5 software (GraphPad Software Inc.; Dotmatics). $P<0.05$ was considered to indicate a statistically significant difference.

Results

Sorafenib and regorafenib trigger an IL-33/ST2L positive feedback loop in senescent HCC cells. Our current findings showed that cisplatin-treated lung cancer cells can release IL-33 to cause an IL-33/ST2L positive feedback loop to limit cisplatin therapeutic efficacy (28). IL-33/ST2L signaling has been implicated in promoting the progression of HCC (26,32). However, whether HCC cells can release IL-33 in response to stress induced by sorafenib and regorafenib remains unclear. To investigate this, Huh-7 cells were treated with various doses of sorafenib and regorafenib. Significant cytotoxicity was observed at concentrations exceeding 20 μM for sorafenib and 40 μM for regorafenib (Fig. 1A). To avoid the passive release of IL-33 due to cell death, Huh-7 cells were treated with 10 μM sorafenib and 20 μM regorafenib in the following experiments. As shown in Fig. 1B, both sorafenib and regorafenib induced the release of IL-33 in Huh-7 cells at 24 and 48 h post-treatment. Interestingly, a notable increase in the cytosolic protein level of IL-33 and the mRNA level of IL-33 was observed in both sorafenib and regorafenib-treated Huh-7 cells (Fig. 1B and C). Since an IL-33 positive feedback loop has been previously identified in macrophages and lung cancer cells (28,33), it was next tested whether this loop occurs in sorafenib and regorafenib-treated Huh-7 cells. To examine this, the mRNA levels of *IL33* and *ST2L* were first measured in recombinant IL-33 (rIL-33)-treated Huh-7 cells. Similar to previous findings, rIL-33 treatment upregulated the mRNA levels of *IL33* and protein levels of surface ST2L in Huh-7 cells (Fig. 1D). Additionally, increased protein levels of IL-33 were also observed following rIL-33 treatment (Fig. 1E). Furthermore, blocking IL-33 signaling with a neutralizing anti-IL-33 (α-IL-33) antibody abolished the upregulation of IL-33 induced by sorafenib and regorafenib in Huh-7 cells (Fig. 1F), indicating that sorafenib and regorafenib trigger an IL-33/ST2L positive feedback loop in HCC cells. Notably, a recent study pointed out that IL-33 was highly induced in senescent hepatic stellate cells within the TME of HCC (27). Given that sorafenib and regorafenib treatment can lead to cellular senescence in HCC cells (34), it was hypothesized that IL-33 is induced in senescent HCC cells triggered by these treatments. To examine whether sorafenib and regorafenib can cause cell growth inhibition, a characteristic of cellular senescence, Huh-7 cells were treated with various concentrations of sorafenib and regorafenib for 24 to 96 h. Significant cell growth arrest was observed in Huh-7 cells treated with 10 μM sorafenib and 20 μM regorafenib (Fig. 2A). Additionally, a significant increase in SA-β-galactosidase expression was observed in sorafenib and regorafenib-treated Huh-7 cells (Fig. 2B). It has been reported that cellular senescence is mainly regulated by $p16^{INK4/CDKN2}$ and $p21^{WAF1/Cip1}$ pathways (35). The present results revealed that sorafenib induced upregulation of p16, while regorafenib increased p21 expression post-treatment compared with the control group (Fig. 2C). These findings collectively indicate that sorafenib and regorafenib trigger an IL-33/ST2L positive feedback loop in senescent HCC cells.

Sorafenib and regorafenib treatments lead to PD-L1 upregulation via IL-33 signaling in HCC cells. It has been reported that IL-33/ST2L signaling can induce PD-L1 expression, leading to immune escape in oral squamous cell carcinoma (36). Notably, elevated PD-L1 expression in patients with HCC correlates with poor survival and resistance to sorafenib (14). It was investigated whether sorafenib and regorafenib treatments increase PD-L1 expression via IL-33 release. As shown in Fig. 3A, both sorafenib and regorafenib enhanced PD-L1 expression on the plasma membrane of Huh-7 cells. Blocking IL-33 signaling with a neutralizing α-IL-33 antibody abolished the upregulation of PD-L1 induced by sorafenib and regorafenib in Huh-7 cells (Fig. 3B), suggesting that IL-33 released from these drug-treated cells induces PD-L1 expression. To further examine whether IL-33 induces PD-L1 upregulation in HCC cells, Huh-7 cells were treated with rIL-33 protein. The immunoblot results revealed that protein levels of PD-L1 increased following stimulation with rIL-33 (Fig. 3C). Additionally, elevated PD-L1 on the surface of rIL-33-treated Huh-7 cells was also detected (Fig. 3D), confirming that IL-33 is capable of inducing PD-L1 expression in HCC cells. The regulation of PD-L1 expression mainly involves the participation of transcriptional regulators, including NF-κB (37). Given that our current findings revealed that NF-κB mediates IL-33-dependent actions in the TME (28), it was examined

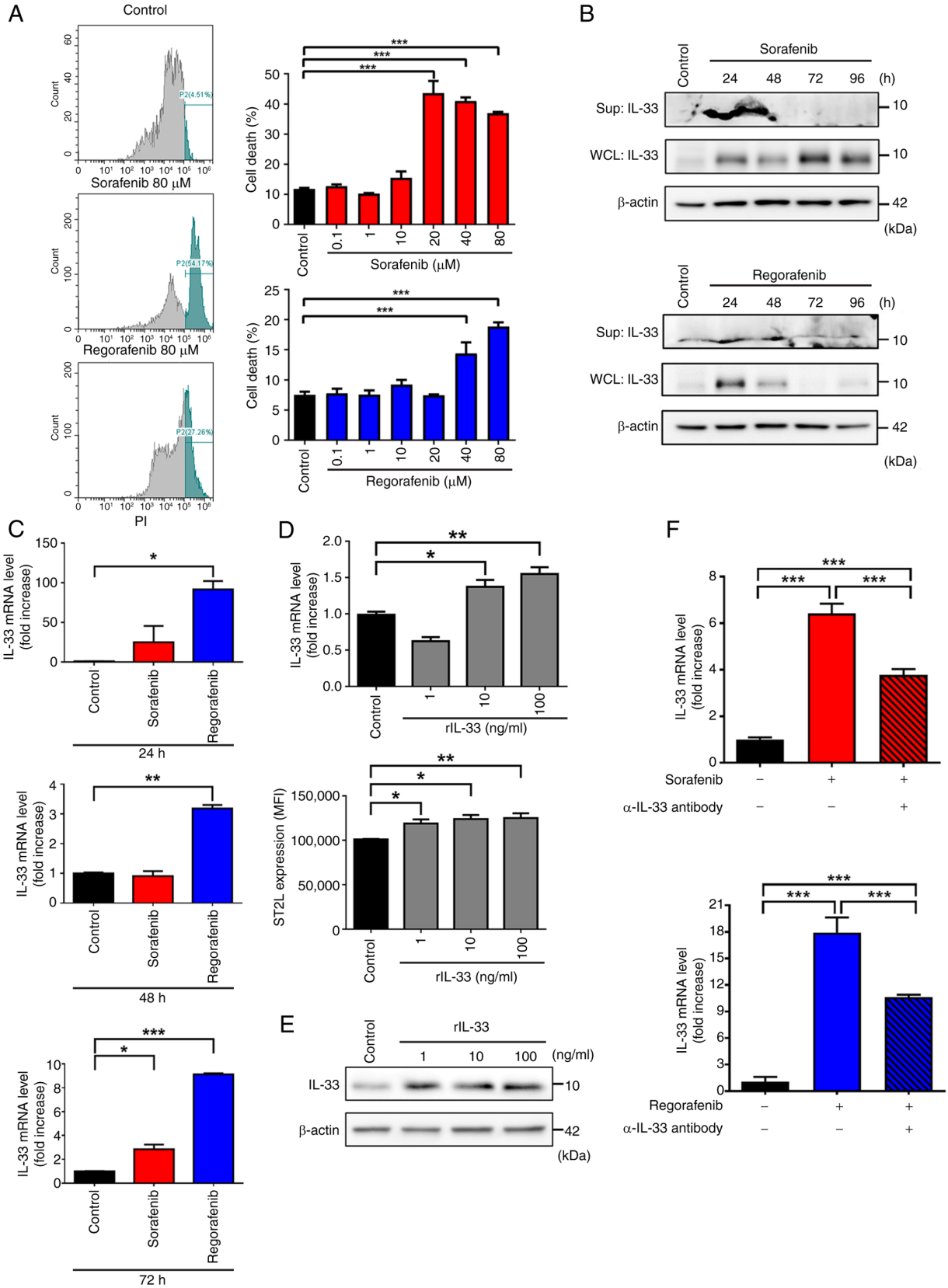

Figure 1. Sorafenib and regorafenib induce IL-33 upregulation and secretion in hepatocellular carcinoma cells. (A) Huh-7 cells were treated with sorafenib or regorafenib at the indicated concentrations. Cell death was assessed using PI staining through flow cytometry. Representative flow cytometry histograms of PI staining in Huh7 cells under the indicated treatment conditions are shown (left). Quantification of PI-positive cells (%) is presented (right). (B and C) Huh-7 cells were treated with DMEM, sorafenib (10 μM), or regorafenib (20 μM) for the indicated time. (B) The protein expression of IL-33 was analyzed by western blotting. (C) The mRNA level of *IL33* was determined by RT-qPCR. (D and E) Huh-7 cells were treated with rIL-33 at the indicated concentrations for 48 h. (D, upper) The mRNA level of *IL33* was determined by RT-qPCR. (D, lower) The cell surface expression of ST2L was measured by flow cytometry. (E) The protein expression of IL-33 was analyzed by western blotting. (F) Huh-7 cells were treated with sorafenib (left) and regorafenib (right) with or without α-IL-33 antibodies (10 μg/ml). The mRNA level of *IL33* was determined by RT-qPCR. *P<0.05, **P<0.01 and ***P<0.001. PI, propidium iodide; RT-qPCR, reverse transcription-quantitative PCR; Sup, supernatant; WCL, whole cell lysate.

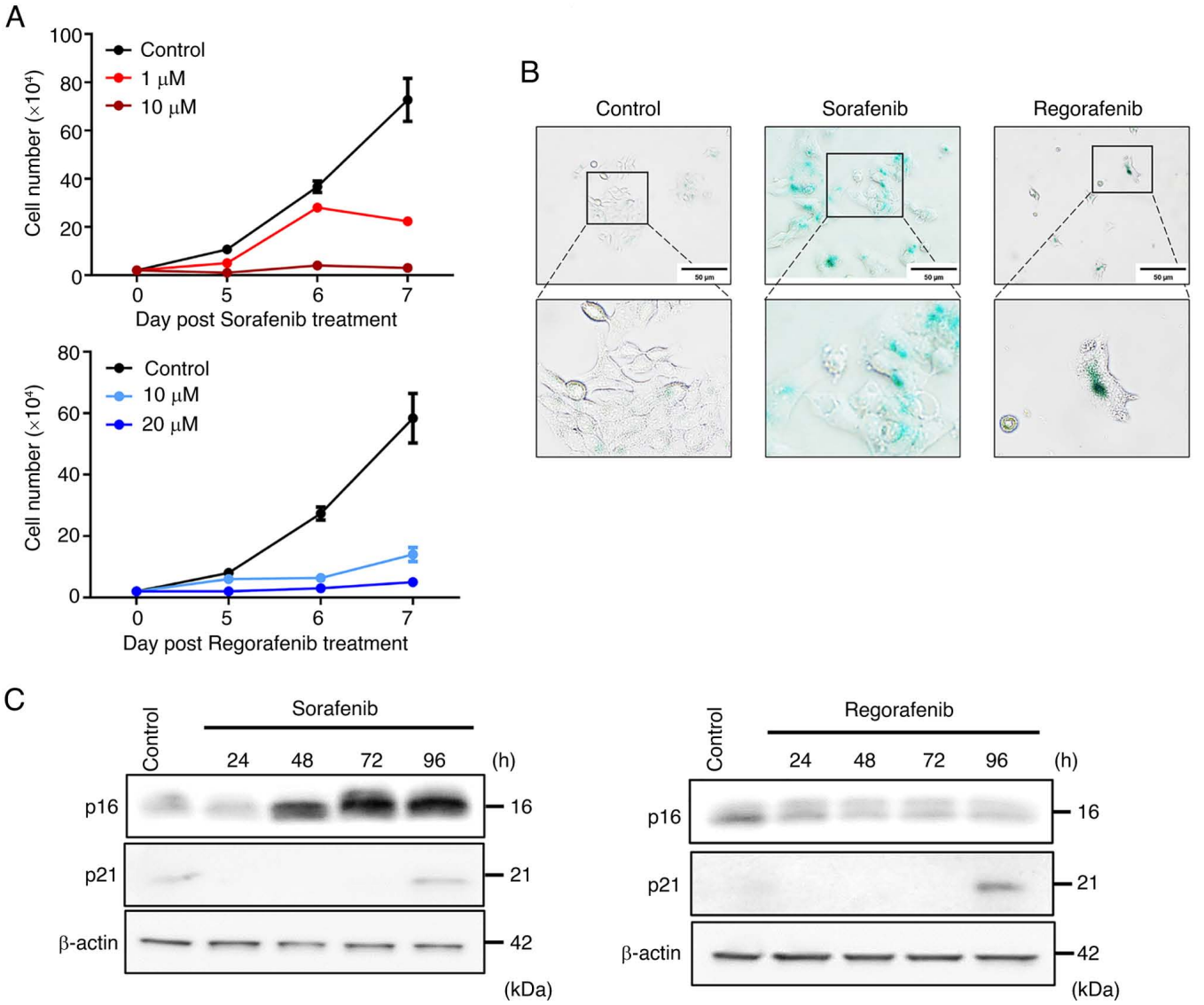

Figure 2. Sorafenib and regorafenib trigger cellular senescence in hepatocellular carcinoma cells. (A) Huh-7 cells were treated with sorafenib (1 and 10 μM, upper) and regorafenib (10 and 20 μM, lower). Cell numbers were calculated using a hemocytometer at the indicated time points. (B) Huh-7 cells were treated with sorafenib (10 μM) and regorafenib (20 μM) for 96 h. The SA-β-gal activity was detected using a senescence detection kit. (C) Huh-7 cells were treated with sorafenib (10 μM, left) and regorafenib (20 μM, right) for the indicated time. The protein expression of p16 and p21 was analyzed by western blotting.

whether IL-33 induced PD-L1 expression via NF-κB in HCC cells. The current data showed that rIL-33-induced upregulation of PD-L1 was significantly abolished in the presence of NF-κB inhibitor (Fig. 3D). These data collectively indicated that sorafenib and regorafenib treatments lead to PD-L1 upregulation via IL-33 signaling in HCC cells.

Blockage of IL-33 or ST2L enhances the antitumor immune responses and therapeutic efficacy of sorafenib in HCC-bearing mice. Next, it was examined whether blocking IL-33/ST2L signaling could enhance the therapeutic efficacy of sorafenib in HCC-bearing mice. To test this hypothesis, low-dose sorafenib treatment (10 mg/kg) (38) was combined with α-IL-33 or α-ST2L neutralizing antibodies (10 mg/kg) in a subcutaneous HCC mouse model by inoculating a mouse HCC cell line ML-1_{5a} in BALB/c mice (39) (Fig. 4A). To assess whether these combination treatments could cause significant toxicity in mice, body weights and serum levels of glutamic oxaloacetic transaminase (GOT), glutamic pyruvic transaminase (GPT), albumin, blood urea nitrogen (BUN) and creatinine were monitored. The results revealed no significant changes in these parameters in mice undergoing the combined treatment compared with control mice (Fig. S1A and B), indicating that no significant toxicity was induced by these treatments. In Fig. 4C, the maximum tumor observed measured 9 mm in length and 13 mm in width, corresponding to a calculated tumor volume of 526.5 mm^3 and a maximum diameter of 13 mm. It was found that single treatments with sorafenib, α-IL-33, or α-ST2L neutralizing antibodies in HCC-bearing mice showed no significant differences in tumor size, growth rate, and weight compared with control groups. Notably, combined treatment with sorafenib and either α-IL-33 or α-ST2L neutralizing antibodies resulted in a remarkable reduction in tumor size, growth rate and weight (Fig. 4B-D). These data indicated that blocking IL-33/ST2L can enhance the antitumor efficacy of sorafenib in HCC. Additionally,

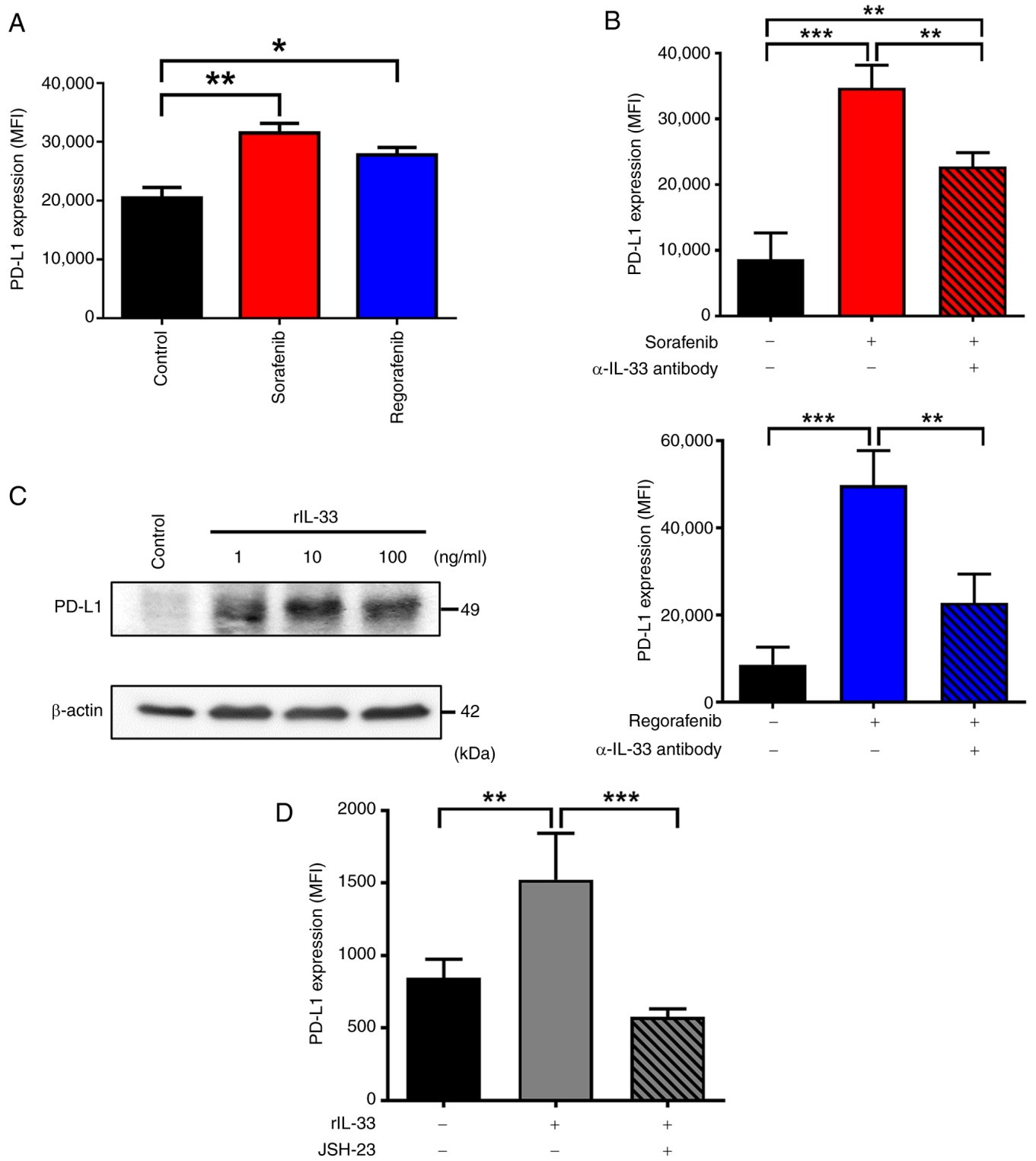

Figure 3. Sorafenib and regorafenib enhance PD-L1 expression via IL-33 signaling in hepatocellular carcinoma cells. (A) Huh-7 cells were treated with sorafenib (10 μM) and regorafenib (20 μM) for 96 h. The cell surface expression of PD-L1 was measured by flow cytometry. (B) Huh-7 cells were treated with sorafenib (10 μM, upper) and regorafenib (20 μM, lower) with or without treatment of α-IL-33 antibodies (10 μg/ml) for 96 h. The cell surface expression of PD-L1 was measured by flow cytometry. (C and D) Huh-7 cells were treated with rIL-33 at the indicated concentrations for 96 h. (C) The mRNA level of *CD274* was determined by reverse transcription-quantitative PCR. (D) Huh-7 cells were treated with rIL-33 (100 ng/ml) with or without treatment of JSH-23 (50 μM). The cell surface expression of PD-L1 was measured by flow cytometry. *P<0.05, **P<0.01 and ***P<0.001. PD-L1, programmed death ligand 1.

consistent with *in vitro* findings, sorafenib treatment induced elevated expression of IL-33 as well as PD-L1 in HCC tumors, which was inhibited by combined treatments with α-IL-33 or α-ST2L neutralizing antibodies (Fig. 4E and F). Given that IL-33/ST2L signaling-induced PD-L1 expression can lead to immune escape (36), the tumor-infiltrating lymphocytes were analyzed 21 days after HCC inoculation. A slight increase was observed in tumor-infiltrating $CD4^{+}$ T cells in HCC tumors

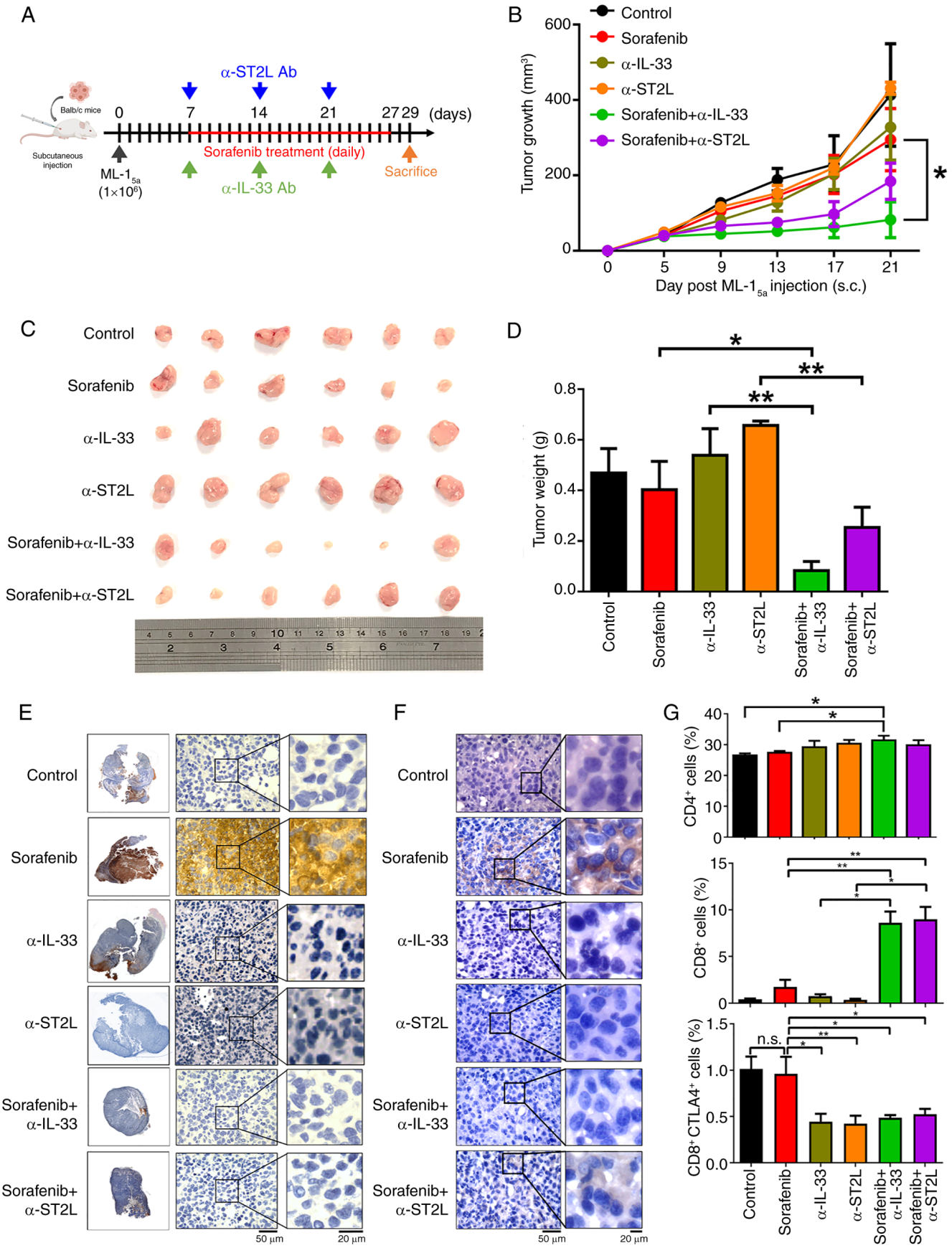

Figure 4. Blockage of IL-33/ST2L by neutralizing antibodies enhances the antitumor efficacy of sorafenib. (A) Schematic illustration of the treatment regimen in the subcutaneous HCC-bearing mouse model. HCC-bearing mice were treated with sorafenib (10 μg/g), α-IL-33 (10 μg/g), α-ST2L (10 μg/g), or a combination of sorafenib with α-IL-33 or α-ST2L. (B) Tumor growth was measured starting from day 5 and once every 4 days. (C and D) Tumor size (C) and tumor weight (D) were measured at the end of the experiment. (E and F) Paraffin-embedded HCC tumor sections from each group were stained with (E) IL-33 and (F) PD-L1 and counterstained with hematoxylin. Magnified views of the inset regions are shown on the right. (G) Intra-tumoral CD4$^+$ T cells (upper), CD8$^+$ T cells (middle), and CD8$^+$CTLA4$^+$ cells (lower) were measured by flow cytometry. HCC, hepatocellular carcinoma. *P<0.05 and **P<0.01.

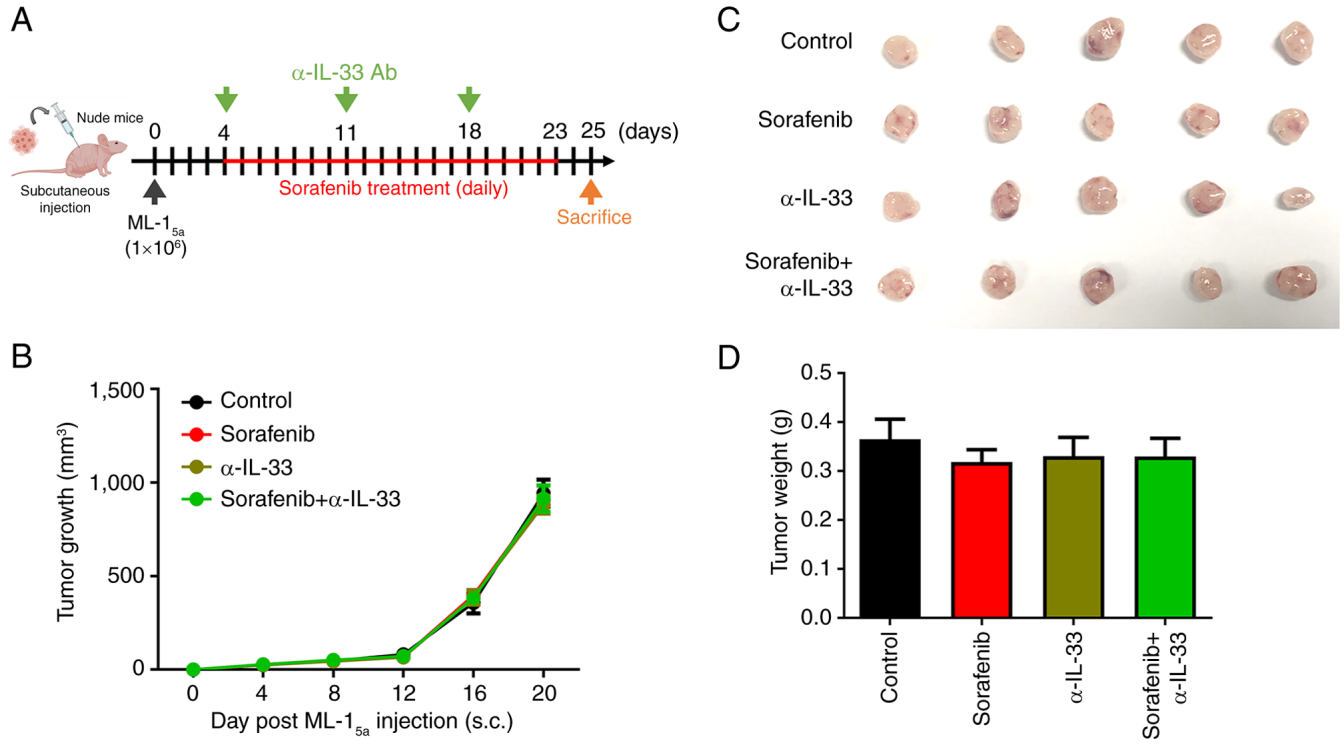

Figure 5. The effectiveness of α-IL-33 neutralizing antibodies in enhancing the antitumor activity of sorafenib is abolished in athymic mice. (A) Schematic illustration of the treatment regimen in the subcutaneous hepatocellular carcinoma-bearing nude mouse model. HCC-bearing nude mice were treated with sorafenib (10 μg/g), α-IL-33 (10 μg/g), or a combination of sorafenib with α-IL-33. (B) Tumor growth was measured starting on day 4 and once every 4 days. (C and D) Tumor size (C) and tumor weight (D) were measured at the end of the experiment.

treated with a combination of sorafenib and α-IL-33 neutralizing antibodies compared with other treatment groups. It is worth noting that a significant increase in tumor-infiltrating $CD8^+$ T cells was observed in HCC tumors treated with sorafenib combined with either α-IL-33 or α-ST2L neutralizing antibodies compared with other treatment groups. Furthermore, a reduction in CTLA4 expression on tumor-infiltrating $CD8^+$ T cells was observed in HCC tumors following treatment with α-IL-33 or α-ST2L neutralizing antibodies (Fig. 4G). These findings suggested that combining sorafenib treatment with α-IL-33 or α-ST2L neutralizing antibodies enhances the activation and infiltration of $CD8^+$ T cells into the TME of HCC tumors, leading to increased therapeutic efficacy of sorafenib.

α-IL-33 neutralizing antibodies enhancing the antitumor activity of sorafenib depend on T cells. Since it was observed that combining sorafenib with an α-IL-33 antibody increased tumor-infiltrated T cells, it was examined whether the α-IL-33 neutralizing antibody enhances the antitumor activity of sorafenib through T cells. To test this hypothesis, an HCC model in nude mice was established by subcutaneously implanting $ML\text{-}1_{5a}$ cells and then treating them with either sorafenib alone or in combination with the α-IL-33 neutralizing antibody (Fig. 5A). The results showed that the combined treatment did not significantly reduce tumor size, growth rate, or tumor weights in the HCC-bearing nude mice compared with the sorafenib-only group (Fig. 5B-D). In Fig. 5C, the largest tumor had a length of 1.3 cm and a width of 1.3 cm, corresponding to a calculated volume of 1,098.5 mm^3. These data suggested that the α-IL-33 neutralizing antibody enhances the antitumor activity of sorafenib by regulating T cell-mediated immunity.

Discussion

When cells experience stress or damage, IL-33 is rapidly released into the cytoplasm, where it serves as an alarmin by binding to ST2L. This IL-33/ST2L interaction has been shown to promote cancer progression, while its role in regulating tumor cell resistance to therapy is just beginning to be investigated. IL-33 has been found to facilitate resistance to Fluorouracil (5-FU) in murine melanoma cells by triggering polyploidy and inducing immune exhaustion (40). Our previous study consistently revealed that IL-33, which is released from lung cancer cells treated with cisplatin, enhances M2 macrophage function, thereby limiting the efficacy of the treatment (28). Additionally, a current study demonstrated that the IL-33/ST2L axis can activate the non-homologous end joining pathway, contributing to DNA damage resistance in lung cancer response to cisplatin or doxorubicin (41). In line with these findings, it was demonstrated that IL-33 plays a significant role in enhancing resistance to the anticancer drugs sorafenib and regorafenib in HCC. Taken together, these results suggest that targeting the IL-33/ST2L pathway could be beneficial in improving the effectiveness of these treatments. While IL-33 can be released from non-necrotic HCC cells in response to sorafenib and regorafenib, little is known about how it is mobilized and released into the extracellular space. Recently, several mechanisms based on non-classical secretion appear to be involved in IL-33 secretion. It has been

found that IL-33 can be cosecreted with exosomes through the neutral sphingomyelinase-2-dependent multivesicular endosome pathway in primary human airway basal cells (42). Additionally, current studies demonstrated that IL-33 release from allergen-stimulated lung epithelial cells and senescent hepatic stellate cells depends on gasdermin D pores, whose generation is independent of or dependent on caspase-1 and caspase-11, respectively (27,43). Understanding whether IL-33 release from sorafenib- and regorafenib-treated HCC cells occurs via gasdermin D pores or exosomal pathways will be important in future studies.

Numerous chemotherapeutic drugs can induce senescence in cancer cells and TME, stimulating immunosurveillance to eliminate tumor cells. However, they can also lead to chronic inflammation and drug resistance, primarily through a set of factors known as senescence-associated secretory phenotypes (SASPs), including pro-inflammatory IL-1 family cytokines (44). In fact, as one of the IL-1 family cytokines, IL-33 has currently been observed in SASPs. For example, IL-33 is released from senescent hepatic stellate cells as the SASPs to promote obesity-associated HCC (27). In radiation-induced skin injury, IL-33 secreted by senescent skin cells inhibits macrophage phagocytosis ability to clear these cells (45). Furthermore, IL-33-induced cellular senescence results in kidney cell damage through the secretion of IL-33-containing SASPs (46). Based on these studies, the present findings suggested that treatments with sorafenib and regorafenib induce cellular senescence in HCC cells and release IL-33 as part of an SASP, which ultimately limits the effectiveness of these drugs. To further investigate the interaction between IL-33 and other SASP factors, the secretion of IL-6, a prominent SASP cytokine, was measured in sorafenib- and regorafenib-treated Huh7 cells. However, it was found that IL-6 levels were below the detection threshold in all groups, indicating that IL-6 might not play a significant role as a SASP factor interacting with IL-33 in our model (Fig. S2). Nevertheless, the potential for IL-33 to cross-talk with other components of the SASPs cannot be ruled out.

Overexpression of PD-L1 is observed in sorafenib-resistant HCC cells and tissues, which is linked to the facilitation of sorafenib resistance (47). Research using sorafenib-resistant HCC cell lines has demonstrated that c-Met upregulates PD-L1 through the MAPK/NF-κB p65 signaling cascade, thereby contributing to sorafenib resistance (48). The elevated levels of PD-L1 can activate the STAT3/DNA methyltransferase 1 pathway to trigger sorafenib resistance or promote epithelial-mesenchymal transition (EMT) in these resistant HCC cell lines (49,50). However, upregulation of PD-L1 is also observed in non-resistant HCC cells upon sorafenib exposure. For example, the induction of PD-L1 and EMT in sorafenib-treated non-resistant HCC cells is reported, while combined inhibition of EMT and PD-L1 enhances the sensitivity of HCC cells to sorafenib (51). In the present study, it was observed that IL-33 mediates the upregulation of PD-L1 in non-resistant HCC cells when exposed to sorafenib and regorafenib. These observations collectively suggest an early induction of PD-L1 expression in HCC cells following these drug treatments. Additionally, our mechanistic study identified a positive feedback loop involving the IL-33/ST2L/NF-κB axis, which contributes to the induction of PD-L1 in HCC cells. Our findings are consistent with earlier observations that IL-33 promotes PD-L1 expression in murine acute myeloid leukemia and oral squamous cell carcinoma (36,52). Importantly, the analysis of data from The Cancer Genome Atlas data on Liver Hepatocellular Carcinoma revealed a significant positive correlation between *IL33* and *CD274* mRNA expression (Spearman's rho=0.349, $P=4.78x10^{-12}$) (Fig. S3). This finding supports the observations of the present study that IL-33 may play a role in inducing PD-L1 upregulation in human HCC. Notably, tumor stromal cells, in addition to tumor cells, have also been shown to produce IL-33. Research has revealed that both IL-33 and its receptor ST2 are highly expressed in the microvascular vessels of the TME in colorectal cancer to regulate tumor angiogenesis and progression (53). Cancer-associated fibroblast-derived IL-33 can promote breast cancer cell metastasis by modifying the immune microenvironment at the metastatic niche toward type 2 inflammation (54). Thus, the current findings do not exclude the possibility of IL-33 produced by tumor-stromal cells due to sorafenib and regorafenib.

The present findings revealed that blocking the IL-33 signaling pathway with anti-IL-33 or anti-ST2L antibodies alongside sorafenib significantly reduced tumor growth in mice with HCC. Notably, this enhanced effect was abolished in athymic nude mice. This suggests that IL-33 promotes the acquired resistance to sorafenib in HCC-bearing mice mainly by regulating immune responses rather than directly affecting HCC cell growth. In fact, accumulated evidence has revealed that the IL-33/ST2 signaling pathway is a potent regulator of the TME. It recruits various immune cell populations that can either promote tumor malignancy or induce tumor regression. This occurs by activating suppressor immune cells, such as tumor-associated macrophages (TAM), regulatory T cells (Tregs), and $CD4^+$ Th2 cells, to inhibit antitumor immunity. Consequently, this pathway plays a significant role in tumor growth and metastasis (55). Notably, current research indicates that sorafenib treatment results in the polarization of TAM into M2 macrophages and promotes Treg differentiation, consequently suppressing the immune response and diminishing the efficacy of sorafenib to HCC (56,57). It will be important in future studies to understand whether IL-33 activates TAM and Tregs to trigger immunosuppressive responses and hence reduce the efficacy of sorafenib and regorafenib to HCC.

HCC is a primary liver cancer that is increasingly common. For patients with advanced HCC, targeted therapies such as sorafenib and regorafenib are recommended. While these treatments can improve survival rates for patients with HCC, the development of acquired resistance often leads to a poor response to these therapies. In the present study, it was revealed that treatments with sorafenib and regorafenib initiate a positive feedback loop involving IL-33 and ST2L in senescent HCC cells. The IL-33 that is secreted enhances the expression of PD-L1 in HCC cells by activating NF-κB pathways in response to these treatments. When the IL-33 signaling pathway was blocked using anti-IL-33 or anti-ST2L antibodies in combination with sorafenib, a significant reduction in tumor growth was observed in mice with HCC. This was accompanied by decreased PD-L1 expression in tumors

and increased infiltration of $CD8^+$ T cells. Importantly, the enhanced efficacy of sorafenib against HCC by inhibiting IL-33 was dependent on T cells. The present findings suggested that IL-33 may diminish the effectiveness of sorafenib and regorafenib, indicating that targeting the IL-33/ST2L axis could improve therapeutic outcomes for HCC. Future studies should extend these findings by evaluating the efficacy and toxicity of IL-33/ST2L inhibitors in higher-order animal models and by investigating their use in combination with other HCC therapies, such as immunotherapy. These approaches will be essential to determine the translational potential of targeting the IL-33/ST2L axis in HCC.

Acknowledgements

Not applicable.

Funding

The present study was supported by the Ministry of Science and Technology of Taiwan (grant nos. MOST 109-2622-B-006-002-CC1 and MOST 110-2622-B-006-006-CC1), the National Science and Technology Council of Taiwan (grant no. NSTC 112-2320-B-006-047) and Chia-Yi Christian Hospital (grant no. CYC111005).

Availability of data and materials

The data generated in the present study may be requested from the corresponding author.

Authors' contributions

YXL and HL confirm the authenticity of all the raw data. YXL, HL, CCC and CPC were responsible for study conception and design, and methodology development. YXL, WCL and BCZ performed the experiments and collected the data. WCL, BCZ, CCC and CPC carried out data analysis and interpretation. YXL, HL, WCL, CCC and CPC wrote and/or revised the manuscript. YCW and SWW provided administrative, technical, or material support and critical revisions. CCC and CPC conducted project administration and overall supervision. All authors read and approved the final version of the manuscript.

Ethics approval and consent to participate

All procedures followed institutional guidelines and were approved by the Institutional Animal Care and Use Committee of National Cheng Kung University (approval no. 107130; Tainan, Taiwan).

Patient consent for publication

Not applicable.

Competing interests

The authors declare that they have no competing interests.

Use of artificial intelligence tools

During the preparation of this work, artificial intelligence tools were used to improve the readability and language of the manuscript or to generate images, and subsequently, the authors revised and edited the content produced by the artificial intelligence tools as necessary, taking full responsibility for the ultimate content of the present manuscript.

References

1. Yang C, Zhang H, Zhang L, Zhu AX, Bernards R, Qin W and Wang C: Evolving therapeutic landscape of advanced hepatocellular carcinoma. Nat Rev Gastroenterol Hepatol 20: 203-222, 2023.
2. Reig M, Forner A, Rimola J, Ferrer-Fàbrega J, Burrel M, Garcia-Criado Á, Kelley RK, Galle PR, Mazzaferro V, Salem R, *et al*: BCLC strategy for prognosis prediction and treatment recommendation: The 2022 update. J Hepatol 76: 681-693, 2022.
3. Wilhelm SM, Carter C, Tang L, Wilkie D, McNabola A, Rong H, Chen C, Zhang X, Vincent P, McHugh M, *et al*: BAY 43-9006 exhibits broad spectrum oral antitumor activity and targets the RAF/MEK/ERK pathway and receptor tyrosine kinases involved in tumor progression and angiogenesis. Cancer Res 64: 7099-7109, 2004.
4. Schroeder B, Li Z, Cranmer LD, Jones RL and Pollack SM: Targeting gastrointestinal stromal tumors: The role of regorafenib. Onco Targets Ther 9: 3009-3016, 2016.
5. Mody K and Abou-Alfa GK: Systemic therapy for advanced hepatocellular carcinoma in an evolving landscape. Curr Treat Options Oncol 20: 3, 2019.
6. Cheng AL, Kang YK, Chen Z, Tsao CJ, Qin S, Kim JS, Luo R, Feng J, Ye S, Yang TS, *et al*: Efficacy and safety of sorafenib in patients in the Asia-Pacific region with advanced hepatocellular carcinoma: A phase III randomised, double-blind, placebo-controlled trial. Lancet Oncol 10: 25-34, 2009.
7. Liu S, Du Y, Ma H, Liang Q, Zhu X and Tian J: Preclinical comparison of regorafenib and sorafenib efficacy for hepatocellular carcinoma using multimodality molecular imaging. Cancer Lett 453: 74-83, 2019.
8. Huang A, Yang XR, Chung WY, Dennison AR and Zhou J: Targeted therapy for hepatocellular carcinoma. Signal Transduct Target Ther 5: 146, 2020.
9. Ladd AD, Duarte S, Sahin I and Zarrinpar A: Mechanisms of drug resistance in HCC. Hepatology 79: 926-940, 2024.
10. Zhang W, Hong X, Xiao Y, Wang H and Zeng X: Sorafenib resistance and therapeutic strategies in hepatocellular carcinoma. Biochim Biophys Acta Rev Cancer 1880: 189310, 2025.
11. Goodman A, Patel SP and Kurzrock R: PD-1-PD-L1 immune-checkpoint blockade in B-cell lymphomas. Nat Rev Clin Oncol 14: 203-220, 2017.
12. Yan F, Pang J, Peng Y, Molina JR, Yang P and Liu S: Elevated cellular PD1/PD-L1 expression confers acquired resistance to cisplatin in small cell lung cancer cells. PLoS One 11: e0162925, 2016.
13. Bishop JL, Sio A, Angeles A, Roberts ME, Azad AA, Chi KN and Zoubeidi A: PD-L1 is highly expressed in enzalutamide resistant prostate cancer. Oncotarget 6: 234-242, 2015.
14. Li D, Sun FF, Wang D, Wang T, Peng JJ, Feng JQ, Li H, Wang C, Zhou DJ, Luo H, *et al*: Programmed death ligand-1 (PD-L1) regulated by NRF-2/MicroRNA-1 regulatory axis enhances drug resistance and promotes tumorigenic properties in sorafenib-resistant hepatoma cells. Oncol Res 28: 467-481, 2020.
15. Kikuchi H, Matsui A, Morita S, Amoozgar Z, Inoue K, Ruan Z, Staiculescu D, Wong JSL, Huang P, Yau T, *et al*: Increased CD8+ T-cell infiltration and efficacy for multikinase inhibitors after PD-1 blockade in hepatocellular carcinoma. J Natl Cancer Inst 114: 1301-1305, 2022.
16. Shigeta K, Matsui A, Kikuchi H, Klein S, Mamessier E, Chen IX, Aoki S, Kitahara S, Inoue K, Shigeta A, *et al*: Regorafenib combined with PD1 blockade increases CD8 T-cell infiltration by inducing CXCL10 expression in hepatocellular carcinoma. J Immunother Cancer 8: e001435, 2020.
17. Li Q, Han J, Yang Y and Chen Y: PD-1/PD-L1 checkpoint inhibitors in advanced hepatocellular carcinoma immunotherapy. Front Immunol 13: 1070961, 2022.

18. Cayrol C and Girard JP: Interleukin-33 (IL-33): A nuclear cytokine from the IL-1 family. Immunol Rev 281: 154-168, 2018.
19. Shlomovitz I, Erlich Z, Speir M, Zargarian S, Baram N, Engler M, Edry-Botzer L, Munitz A, Croker BA and Gerlic M: Necroptosis directly induces the release of full-length biologically active IL-33 in vitro and in an inflammatory disease model. FEBS J 286: 507-522, 2019.
20. Cayrol C and Girard JP: IL-33: An alarmin cytokine with crucial roles in innate immunity, inflammation and allergy. Curr Opin Immunol 31: 31-37, 2014.
21. Cayrol C: IL-33, an alarmin of the IL-1 family involved in allergic and non allergic inflammation: Focus on the mechanisms of regulation of its activity. Cells 11: 107, 2021.
22. Weber A, Wasiliew P and Kracht M: Interleukin-1 (IL-1) pathway. Sci Signal 3: cm1, 2010.
23. Griesenauer B and Paczesny S: The ST2/IL-33 axis in immune cells during inflammatory diseases. Front Immunol 8: 475, 2017.
24. Pisani LF, Teani I, Vecchi M and Pastorelli L: Interleukin-33: Friend or foe in gastrointestinal tract cancers? Cells 12: 1481, 2023.
25. Zhao R, Yu Z, Li M and Zhou Y: Interleukin-33/ST2 signaling promotes hepatocellular carcinoma cell stemness expansion through activating c-Jun N-terminal kinase pathway. Am J Med Sci 358: 279-288, 2019.
26. Wang W, Wu J, Ji M and Wu C: Exogenous interleukin-33 promotes hepatocellular carcinoma growth by remodelling the tumour microenvironment. J Transl Med 18: 477, 2020.
27. Yamagishi R, Kamachi F, Nakamura M, Yamazaki S, Kamiya T, Takasugi M, Cheng Y, Nonaka Y, Yukawa-Muto Y, Thuy LTT, *et al*: Gasdermin D-mediated release of IL-33 from senescent hepatic stellate cells promotes obesity-associated hepatocellular carcinoma. Sci Immunol 7: eabl7209, 2022.
28. Yang YE, Hu MH, Zeng YC, Tseng YL, Chen YY, Su WC, Chang CP and Wang YC: IL-33/NF-κB/ST2L/Rab37 positive-feedback loop promotes M2 macrophage to limit chemotherapeutic efficacy in lung cancer. Cell Death Dis 15: 356, 2024.
29. Chen SH, Hu CP, Lee CK and Chang C: Immune reactions against hepatitis B viral antigens lead to the rejection of hepatocellular carcinoma in BALB/c mice. Cancer Res 53: 4648-4651, 1993.
30. Livak KJ and Schmittgen TD: Analysis of relative gene expression data using real-time quantitative PCR and the 2(-Delta Delta C(T)) method. Methods 25: 402-408, 2001.
31. Li T, Fu J, Zeng Z, Cohen D, Li J, Chen Q, Li B and Liu XS: TIMER2.0 for analysis of tumor-infiltrating immune cells. Nucleic Acids Res 48 (W1): W509-W514, 2020.
32. Pan X, Liu J, Li M, Liang Y, Liu Z, Lao M and Fang M: The association of serum IL-33/ST2 expression with hepatocellular carcinoma. BMC Cancer 23: 704, 2023.
33. Akimoto M, Hayashi JI, Nakae S, Saito H and Takenaga K: Interleukin-33 enhances programmed oncosis of ST2L-positive low-metastatic cells in the tumour microenvironment of lung cancer. Cell Death Dis 7: e2057, 2016.
34. Wang C, Wang H, Lieftink C, du Chatinier A, Gao D, Jin G, Jin H, Beijersbergen RL, Qin W and Bernards R: CDK12 inhibition mediates DNA damage and is synergistic with sorafenib treatment in hepatocellular carcinoma. Gut 69: 727-736, 2020.
35. Roger L, Tomas F and Gire V: Mechanisms and regulation of cellular senescence. Int J Mol Sci 22: 13173, 2021.
36. Zhao M, He Y, Zhu N, Song Y, Hu Q, Wang Z, Ni Y and Ding L: IL-33/ST2 signaling promotes constitutive and inductive PD-L1 expression and immune escape in oral squamous cell carcinoma. Br J Cancer 128: 833-843, 2023.
37. Lin X, Kang K, Chen P, Zeng Z, Li G, Xiong W, Yi M and Xiang B: Regulatory mechanisms of PD-1/PD-L1 in cancers. Mol Cancer 23: 108, 2024.
38. Jian C, Fu J, Cheng X, Shen LJ, Ji YX, Wang X, Pan S, Tian H, Tian S, Liao R, *et al*: Low-dose sorafenib acts as a mitochondrial uncoupler and ameliorates nonalcoholic steatohepatitis. Cell Metab 31: 1206, 2020.
39. Shiau DJ, Kuo WT, Davuluri GVN, Shieh CC, Tsai PJ, Chen CC, Lin YS, Wu YZ, Hsiao YP and Chang CP: Hepatocellular carcinoma-derived high mobility group box 1 triggers M2 macrophage polarization via a TLR2/NOX2/autophagy axis. Sci Rep 10: 13582, 2020.
40. Kudo-Saito C, Miyamoto T, Imazeki H, Shoji H, Aoki K and Boku N: IL33 is a key driver of treatment resistance of cancer. Cancer Res 80: 1981-1990, 2020.
41. Luo H, Liu L, Liu X, Xie Y, Huang X, Yang M, Shao C and Li D: Interleukin-33 (IL-33) promotes DNA damage-resistance in lung cancer. Cell Death Dis 16: 274, 2025.
42. Katz-Kiriakos E, Steinberg DF, Kluender CE, Osorio OA, Newsom-Stewart C, Baronia A, Byers DE, Holtzman MJ, Katafiasz D, Bailey KL, *et al*: Epithelial IL-33 appropriates exosome trafficking for secretion in chronic airway disease. JCI Insight 6: e136166, 2021.
43. Chen W, Chen S, Yan C, Zhang Y, Zhang R, Chen M, Zhong S, Fan W, Zhu S, Zhang D, *et al*: Allergen protease-activated stress granule assembly and gasdermin D fragmentation control interleukin-33 secretion. Nat Immunol 23: 1021-1030, 2022.
44. Dong Z, Luo Y, Yuan Z, Tian Y, Jin T and Xu F: Cellular senescence and SASP in tumor progression and therapeutic opportunities. Mol Cancer 23: 181, 2024.
45. Liu G, Chen Y, Dai S, Wu G, Wang F, Chen W, Wu L, Luo P and Shi C: Targeting the NLRP3 in macrophages contributes to senescence cell clearance in radiation-induced skin injury. J Transl Med 23: 196, 2025.
46. Chen L, Gao C, Yin X, Mo L, Cheng X, Chen H, Jiang C, Wu B, Zhao Y, Li H, *et al*: Partial reduction of interleukin-33 signaling improves senescence and renal injury in diabetic nephropathy. MedComm (2020) 5: e742, 2024.
47. Zhang J, Zhao X, Ma X, Yuan Z and Hu M: KCNQ1OT1 contributes to sorafenib resistance and programmed death-ligand-1-mediated immune escape via sponging miR-506 in hepatocellular carcinoma cells. Int J Mol Med 46: 1794-1804, 2020.
48. Xu R, Liu X, Li A, Song L, Liang J, Gao J and Tang X: c-Met up-regulates the expression of PD-L1 through MAPK/NF-κBp65 pathway. J Mol Med (Berl) 100: 585-598, 2022.
49. Liu J, Liu Y, Meng L, Liu K and Ji B: Targeting the PD-L1/DNMT1 axis in acquired resistance to sorafenib in human hepatocellular carcinoma. Oncol Rep 38: 899-907, 2017.
50. Xu GL, Ni CF, Liang HS, Xu YH, Wang WS, Shen J, Li MM and Zhu XL: Upregulation of PD-L1 expression promotes epithelial-to-mesenchymal transition in sorafenib-resistant hepatocellular carcinoma cells. Gastroenterol Rep (Oxf) 8: 390-398, 2020.
51. Shrestha R, Prithviraj P, Bridle KR, Crawford DHG and Jayachandran A: Combined inhibition of TGF-β1-induced EMT and PD-L1 silencing re-sensitizes hepatocellular carcinoma to sorafenib treatment. J Clin Med 10: 1889, 2021.
52. Qin L, Dominguez D, Chen S, Fan J, Long A, Zhang M, Fang D, Zhang Y, Kuzel TM and Zhang B: Exogenous IL-33 overcomes T cell tolerance in murine acute myeloid leukemia. Oncotarget 7: 61069-61080, 2016.
53. Cui G, Qi H, Gundersen MD, Yang H, Christiansen I, Sørbye SW, Goll R and Florholmen J: Dynamics of the IL-33/ST2 network in the progression of human colorectal adenoma to sporadic colorectal cancer. Cancer Immunol Immunother 64: 181-190, 2015.
54. Shani O, Vorobyov T, Monteran L, Lavie D, Cohen N, Raz Y, Tsarfaty G, Avivi C, Barshack I and Erez N: Fibroblast-derived IL33 Facilitates breast cancer metastasis by modifying the immune microenvironment and driving type 2 immunity. Cancer Res 80: 5317-5329, 2020.
55. Yeoh WJ, Vu VP and Krebs P: IL-33 biology in cancer: An update and future perspectives. Cytokine 157: 155961, 2022.
56. Yang Q, Cui M, Wang J, Zhao Y, Yin W, Liao Z, Liang Y, Jiang Z, Li Y, Guo J, *et al*: Circulating mitochondrial DNA promotes M2 polarization of tumor associated macrophages and HCC resistance to sorafenib. Cell Death Dis 16: 153, 2025.
57. Shen Y, Wang H, Ma Z, Hao M, Wang S, Li J, Fang Y, Yu L, Huang Y, Wang C, *et al*: Sorafenib promotes treg cell differentiation to compromise its efficacy via VEGFR/AKT/Foxo1 signaling in hepatocellular carcinoma. Cell Mol Gastroenterol Hepatol 19: 101454, 2025.